

Automatic Microtitrator for Small Volume Samples

Zhizhen Wu, Abid Rehman, Zhehao Zhang, and Ian Papautsky*

Cite This: *ACS Meas. Sci. Au* 2022, 2, 430–438

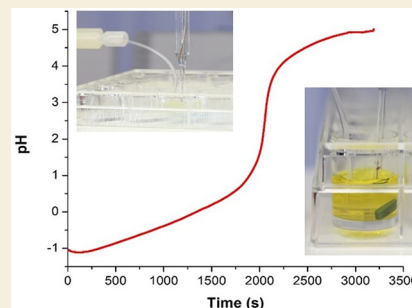
Read Online

ACCESS |

Metrics & More

Article Recommendations

ABSTRACT: Electroanalytical sensors for point-of-care biomedical or point-of-use environmental sample analysis are gaining popularity due to low limits of detection, ease of miniaturization, convenience, and ability to work with small sample volumes. Since pH must be tightly controlled for optimum electrochemical performance, adjustment of pH in these samples is often a necessity. Yet manual titration is time-consuming and can be especially challenging for small volumes. End point determination can also be difficult. Current commercial automatic pH titrators are generally designed for large volume (>1 mL) batch titrations, while the existing microvolume titrators are semiautomatic at best, still relying on multiple manual steps. To address the gap, we developed an automatic microtitration system suitable for small volume samples. The system was validated using digested whole blood microsamples, successfully demonstrating accurate and rapid pH adjustment for samples as small as 100 μL . The simple modular construction of the system makes it compatible with acid washing for trace metal detection and other cleaning or sample preparation steps. The electrochemical detection of manganese heavy metal in blood at the parts per billion level showed no detectable contamination induced by the system. Ultimately, our simple, accurate, user-friendly automatic microtitration system can be used in the pH adjustment of microvolume samples and can potentially be extended to other pH end point analysis.



KEYWORDS: *Microtitration, small volume samples, microvolume titrator, automated pH adjustment, acid-based titration, trace level analysis*

1. INTRODUCTION

The analytical laboratory approaches used to measure trace metals in water or biological samples are generally based on either spectrometry (e.g., ICP-MS)^{1,2} or spectroscopy (e.g., AAS).^{3,4} These techniques are widely used due to high accuracy and sensitivity and low limits of detection at the sub-parts per billion level.⁵ However, the high cost of instrumentation, the need for highly trained personnel, and the use of relatively large sample volumes (mL) has led to growing interest in electroanalytical methods for point-of-care biomedical or point-of-use environmental applications. Many point-of-care sensors and analysis methods rely on small sample volumes collected.^{6–13} These are typically biofluids such as blood or sweat or saliva. Frequently, the pH of these samples must be adjusted, especially if the samples undergo acidification to break up biological components, such as protein and cells, for the electrochemical measurements.¹⁴ Traditionally, this process involves manual pipetting of the titrant into the solution. However, the manual titration is time-consuming and can be challenging for small volumes. Further, pH adjustment is a highly nonlinear process and pH can change drastically after the equivalence point.¹⁵ It is also difficult to determine when the end point is reached, leading to overtitrating and passing the end point. Commercial titrators^{16–18} are not suitable for this, since they are designed

to work with larger sample volumes and at high titrating flows (>100 $\mu\text{L}/\text{min}$) for batch titrations.

For titration of small sample volumes (<500 μL), several methods have been developed for in situ measurement applications, e.g., buret-based systems using fused silica capillaries and spectrophotometric end point detection systems. These can reduce sample volume down to below 250 μL .^{19,20} A spectroscopic method was introduced by optically monitoring the indicator color change of acid–base end point titrations.²¹ Van der Schoot et al.²² further reported on automated colorimetric titration systems, which are advantageous due to the high reproducibility and accuracy of diffusion driven microtitrators. For point-of-care electrochemical sensors, the relative pH change is monitored to accurately determine the end point of titration reactions. The pH can easily be measured in situ with potentiometric microelectrodes. For example, Steinsberger et al.²³ demonstrated a RuO₂ electrode for pH measurements, while Chen et al.²⁴ reported an IrO_x electrode. Nevertheless, many point-of-

Received: April 19, 2022

Revised: June 28, 2022

Accepted: June 29, 2022

Published: July 14, 2022



care systems work with miniscule sample volumes, such as drops of blood. While measurement of pH is such small volumes can be done with the aforementioned probes, adjustment of pH in these microvolume samples remains challenging. Hence, an automated titration method capable of working with minimal sample volumes is very desirable.

In this work, we report on a simple approach for automatic pH titration in microvolume samples. The system relies on a microscale pH probe for feedback and end point measurement. Feedback is used to adjust titration flow, with a fuzzy logic controller used to make these adjustments. The approach was validated and applied to electrochemical determination of Mn in human blood. A blood digestion protocol is necessary to fully decomplex Mn bound to protein, which yields samples at $\text{pH} < -1$ due to acidification with nitric acid. Since cathodic stripping voltammetry (CSV) for Mn determination is performed at $\text{pH} 5.0$, an adjustment with minimal dilution is necessary. Herein, we demonstrate that the developed pH microtitrator is capable of rapid and autonomous titration of these samples.

2. EXPERIMENTAL SECTION

2.1. Reagents

Nitric acid (67%, TraceMetal grade) and sodium hydroxide monohydrate (TraceSELECT grade) were purchased from Fisher Scientific. Hydrogen peroxide (30%) for ultratrace analysis was purchased from Sigma-Aldrich. A 5.0 M sodium hydroxide solution was prepared by dissolving 2.9 g of sodium hydroxide in 10 mL of deionized (DI) water. A 0.1 M sodium acetate buffer was prepared by dilution from a stock solution of 3.0 M, $\text{pH} 5.2 \pm 0.1$ sodium acetate (Sigma-Aldrich). Mn solutions of desired concentrations were prepared from atomic absorption standard solution of $1000 \text{ mg L}^{-1} \text{ Mn}^{2+}$ in 2–5% HNO_3 (Acros Organics).

2.2. System Components

The system consisted of a syringe pump used to dispense sodium hydroxide for pH adjustment and a miniature pH probe for feedback. Figure 1a illustrates the setup. The 5 mL syringes (ALS, Norm-Ject) were purchased from Air-Tite Products Co. The syringe was connected to 0.02" id/0.04" od (0.5 mm id/1 mm od) Tygon tubing purchased from Cole-Parmer. The connections were made with luer lock adapters (P-618, P-620) purchased from IDEX Health & Science. All of the fluidic components of the system were acid washed in 10% nitric acid by overnight soaking and rinsed thoroughly in DI water. Once clean, components were assembled and 5 M NaOH was loaded in the syringe. A syringe pump (1000X, New Era) was used to house and drive the syringe. A miniature pH probe (MI-410, Microelectrodes Inc.) was connected to pH meter (Denver Instruments, model 225) to provide feedback.

Both the syringe pump and the pH meter were controlled using LabView software (NI, v2015). A fuzzy logic controller was implemented to dynamically control the dispense rate and make adjustments based on pH sensor readouts. For pH adjustment, samples were pipetted into wells of 24-, 48-, or 96-well microplates, depending on sample size. The microplate was positioned on a stirring plate, and micro stir bars were used for agitation. Sample volume was inputted into the control software via user interface. The interface window displays the dynamic plot of pH vs time, the real-time pH value, the status of the syringe pump (stop, infuse, withdraw, pause), the flow rate of the syringe pump, and the total infused volume. These data are recorded and stored at a rate of 1 Hz.

2.3. Controller Structure

The implemented fuzzy logic controller (FLC) consisted of three major steps: fuzzification, fuzzy inference system, and defuzzification. During fuzzification, the process variable (PV), which is the "crisp" input, was decomposed as a linear combination of input sets by using

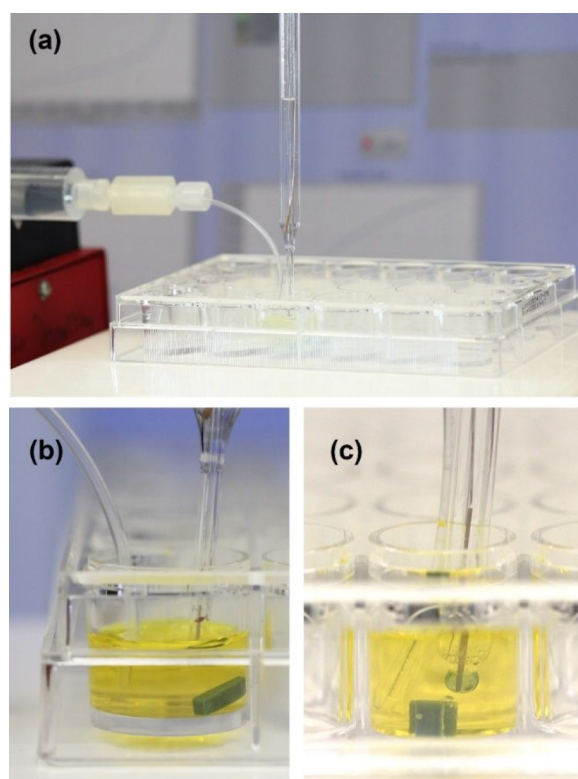


Figure 1. Photographs of the automatic pH adjustment system. (a) Microtitrator system during pH adjustment in a 24-well microplate, with the LabView fuzzy controller visible in the background. (b) Close-up photograph of a microvolume sample during pH adjustment in a 24-well microplate (12 mm well diameter). (c) Close-up photograph of a microvolume sample during pH adjustment in a 96-well microplate (5 mm well diameter).

membership functions (MF) (Figure 2a). Each membership function can take either a Gaussian, triangular, trapezoidal, sigmoid, or piecewise linear shape. Both the shape and boundaries of each membership function can be determined either heuristically or algorithmically via tools such as genetic algorithms. The fuzzy inference system is the process by which the "fuzzy" inputs are turned into "fuzzy" outputs. Using a rules base, as shown in Figure 2b, each fuzzy input was mapped to a corresponding fuzzy output. Defuzzification is the step in which "fuzzy" outputs are converted into a "crisp" output using output membership functions (Figure 2a). Similar to input membership functions, output membership functions can have a variety of both shapes and boundaries. Once more, these shapes and boundaries can be determined either heuristically or via algorithmic tuning methods. Through these steps, human thinking is mimicked.²⁵ As such, the input variables for the FLC should reflect the variables an expert operator will consider when titrating. A typical human operator will likely account for both the pH of the system, as well as the initial volume of the sample when titrating. Therefore, these input variables were used in the titration process. Figure 2c shows the resultant fuzzy logic output space with the given input variables. The variable, "difference," represents the pH difference between the real-time pH value and the preset end point. The variable "volume," represents the initial volume of the sample, and the output variable, "rate," represents the flow rate. However, the initial volume of the sample typically only has a significant effect on the early stages of the titration. Thus, our inference system can be simplified such that the initial volume of the sample only affects the flow rate when the pH is low (<0).

2.4. Titration Experiments

Titration experiments were carried out with digested blood samples we use for electrochemical determination of Mn. The procedure for

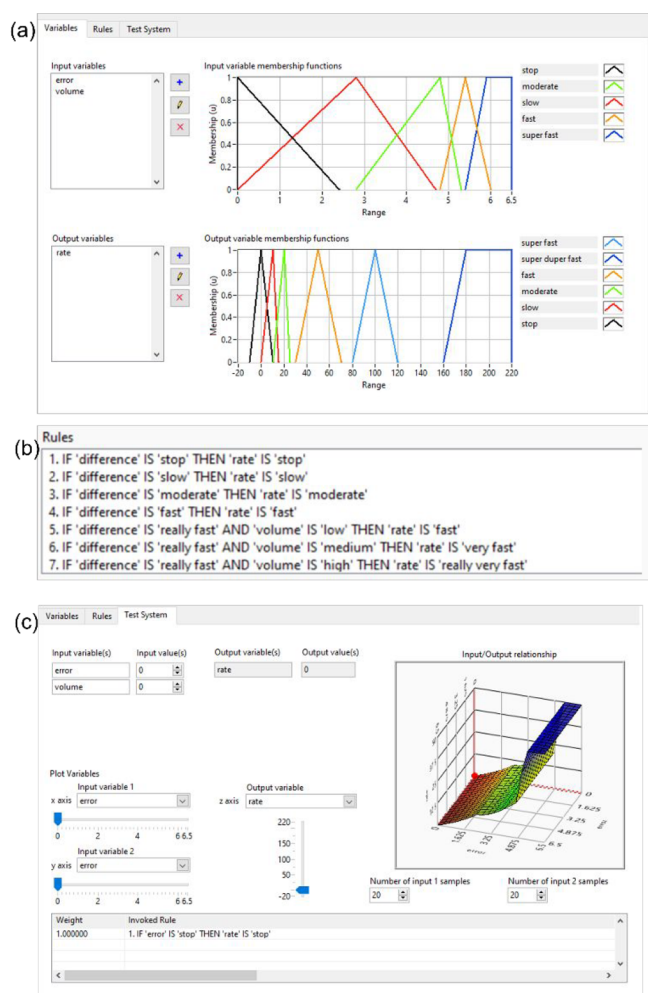


Figure 2. A fuzzy logic controller implemented to control titrant dispense rate during pH adjustment. (a) Structure of the fuzzy logic controller, (b) rules base of the fuzzy logic controller, and (c) resultant fuzzy logic output space with the given input variables.

these experiments was similar to our previous work.²⁶ Sample preparation included microwave digestion of whole blood, which was performed using the Discover SP-D Clinical microwave digestion system (CEM Inc.). For this, a 0.25 mL whole blood sample was pipetted into a 10 mL quartz digestion vial, followed by addition of 0.5 mL of HNO₃ and 0.25 mL of H₂O₂. The sample solution was mixed in the vial by gentle agitation. The vial was sealed with a PTFE cap and digested at 200 °C with 7 min ramp up, 3 min hold time, and 300 psi maximum pressure. The digested blood sample was then pipetted into wells on the microplates.

To test the pH adjustment capability of the system, different volumes (100, 150, 250, 500, and 1000 μ L) of digested blood were used. A 96-well microplate was used for 100 μ L samples, 48-well microplate for 150 and 250 μ L samples, and 24-well microplate for 500 and 1000 μ L samples. The microplate with the blood sample was placed on a stirring plate, and a micro-stir bar was used at 800 rpm to ensure quick mixture of the blood sample and the titrated NaOH. The pH microprobe and the tip of the Tygon tubing were then immersed into the digested blood sample. A 5 min rest time was used for the pH microprobe to stabilize. The pH adjustment process was then initiated using “start” button on the software user interface. NaOH was continuously titrated into the digested blood sample until the pH value reached the preset end point.

After obtaining the pH adjusted sample, electrochemical measurements of manganese (Mn) in the blood sample using our previously reported method were performed.²⁶ ITO was used as the working

electrode, while Ag/AgCl and carbon paste were used as the reference electrode and auxiliary electrode, respectively. Square wave cathodic stripping voltammetry (CSV) was used for Mn determination to achieve low limits of detection. During measurement, the working electrode was biased at a positive potential of 1.2 V to deposit insoluble MnO₂ on the electrode surface by oxidizing Mn²⁺ for 15 min. When the preconcentration step was complete, the electrode potential was swept negatively from 1.2 to 0 V to reduce insoluble MnO₂ back to Mn²⁺ and strip it off the surface, with the waveform parameters of 70 ms period, 5 mV increment, and 25 mV amplitude. The cathodic current was measured and correlated to the concentration of Mn²⁺ in the solution. A standard addition method was used to minimize impact of sample matrix of the blood sample. For validation, Mn measurements were also performed in the same digested blood samples but with manually adjusted pH. For the manual pH adjustment, 5 M NaOH was carefully pipetted into the digested blood with a pipet and metal-free pipet tips (Cole-Palmer) until pH reached 5. The results of the manually adjusted and auto-adjusted blood samples were compared using a *t* test (*p* < 0.05).

3. RESULTS AND DISCUSSION

3.1. System Design and Operation

Our microtitrator system is composed of a syringe pump used to dispense the titrant (in our case, 5 M NaOH) solution for pH adjustment and a miniature pH probe for feedback and end point determination. Figure 1a illustrates the setup. We selected 5 mL Norm-Ject syringes (Air-Tite Products Co.) for this work as they are manufactured from laboratory grade polypropylene and contain no rubber, latex, silicone oil, or styrene. These syringes are a good choice for applications needing an inert, nonreactive syringe. Polypropylene is resistant to nitric acid and thus can be acid-washed for trace metal applications. The low cost and disposable nature of the syringes make them a convenient choice for this application. Small-bore Tygon tubing is used to dispense the titrant directly into the sample microwell of a microplate. While a variety of metal and plastic tips with a Luer lock interface could be used for the dispensing end, we opted for the simplest solution of using tubing only. This approach also prevents any metal contamination for trace analysis and allows all of the fluidic components to be acid-washed.

While a wide range of commercially available microcentrifuge tubes can be used to contain the samples, in our experience microplates are the most convenient as they can be used for single or batch sample titrations. Microplates are readily available in a wide range of sizes and materials, including polypropylene, and thus can be acid-washed for trace metal analysis. Selection of the microplate is dependent on the sample volume and the expected dilution during the titration process, with the largest 6-well microplates accommodating up to 5 mL of liquid and the smallest 384-well microplates accommodating up to 100 μ L of liquid. In this work, we used the 24-well microplates for 0.5–1 mL samples (Figure 1b), the 48-well microplates for 150–250 μ L samples, and the 96-well microplates for 100 μ L samples (Figure 1c). The 5 mm well diameter of the 96-well microplate was the smallest practical size that could accommodate the tubing, pH probe, and micro-stir bar.

Accurate measurement of sample pH is especially critical in our system, since it controls the dispensing rate of the titrant and determines the process end point. Sample pH can be accurately measured in small volumes by integrating metal oxide electrodes in microfluidic channels. For example, Steinsberger et al. demonstrated a RuO₂ electrode for pH

measurements,²³ while Chen et al. reported an IrO_x electrode.²⁴ However, while we have used a similar approach in the past with ion selective electrodes,²⁷ adopting this approach herein would necessitate the use of custom microfluidic cells and would make the instrument setup more complex. The titration process end point determination can be also done spectrometrically using a combination of an LED and a photodiode.^{20,28,29} This approach, however, also requires the development of custom flow cell setups and integration with optical devices. Thus, we selected a microelectrode-type probe for measurement of pH instead, as it allowed for not only determination of the end point of the titration but also monitoring of the process and providing feedback to the software controller. In addition, the small size of the probe (tip outer diameter \sim 1.25 mm) permitted measurements in sample microvolumes inside the 5 mm diameter wells of a 96-well microplate.

Generating a homogeneous mixture of the sample solution and titrant is critically important to ensuring accurate pH measurements. The reaction kinetics are often impacted by mass transport, which is a combination of both diffusion and advection processes. The latter arises from flow, while the former is driven by concentration gradients and generally is the slower of the two. The most prevalent advection-generating system for microplates is an orbital shaker, as they are easy to use and require little supervision. However, shaker-induced advection relies on sloshing of the liquid, which can translate into nonuniform kinetics and thus inconstant results, as recently discussed by Pereiro et al.³⁰ Our own work with agitation of samples for point-of-care electrochemical measurements shows that while measurements can be performed in acquiescent microvolumes, agitating them with vibration can substantially decrease equilibration (mixing) time and improve signal.^{8,31,32} Yet vibration stages can introduce mechanical noise that manifests in noisy voltammograms and thus greater measurement variability. Thus, we opted to use a magnetic micro-stir bar inside the microplate wells to provide continuous agitation and to ensure accurate pH measurements during the entire titration process. This was especially important when working with microvolume samples, as rapid and accurate pH readings help prevent overshooting of the end point.

A photograph of the representative user interface of the fuzzy control system during measurement is illustrated in Figure 3. The interface provides user feedback on the real-time pH value, the real time titrant flow rate, the pH vs time plot, the total volume of titrant dispensed, and the syringe (dispensing) status. These data can then be saved for documentation or further analysis, as we show below.

We used digested blood samples to demonstrate system operation during pH adjustment. Due to addition of nitric acid during the digestion process, pH of the digested blood samples is typically negative, pH < -1. However, the electrochemical measurements generally need an optimal pH value for the best performance,^{8,26,31,33} which makes pH adjustment necessary. In our previous work on manganese determination in blood by cathodic stripping voltammetry,²⁶ we tested samples with pH in the 3.0 to 7.0 range. Solutions with acidic pH prevented Mn²⁺ oxidation, while solutions with higher pH yielded formation of insoluble manganese hydroxides that precipitated, also deterring oxidation of Mn²⁺. The optimization results showed that a weakly acidic solutions at pH 5.0–6.0 yielded the highest stripping signal. Here, a 2 mL digested blood

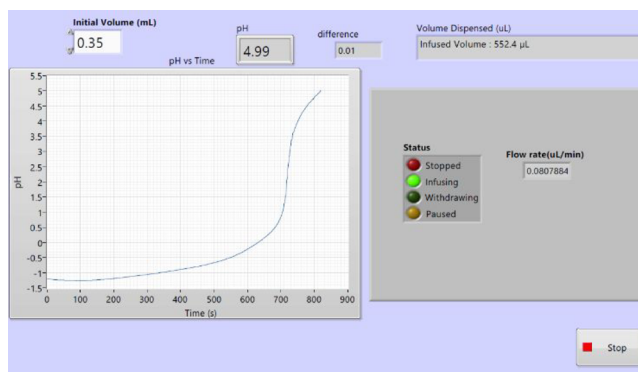


Figure 3. Photograph of the representative user interface of the fuzzy control system during measurement. The interface provides user feedback on the real-time pH value, the real time titrant flow rate, the pH vs time plot, the total volume of titrant dispensed, and the syringe (dispensing) status.

sample was titrated with 5 M NaOH to the end point of pH = 5. During the titration process, sample pH, titrant flow rate, and total volume of infused titrant were recorded at the rate of 1 Hz. The results in Figure 4a show that the pH of the digested blood sample continuously increased from -1.2 to the preset end point of 5 over the course of approximately 75 min. The titrant flow rate data in Figure 4b show that the flow rate begins at the preset starting value of 100 μ L/min and gradually decreases as the process proceeds and sample pH approaches the end point. The flow rate ends at 0.5 μ L/min when the titration reaches the target pH value. Presenting flow rate data as a function of pH in Figure 4c further illustrates how feedback data from the pH probe is used to continuously adjust the flow rate down as not to overshoot the target value. As pH is the negative decadic logarithm of the molar hydrogen ion concentration, the pH change with the NaOH volume is extremely nonlinear. Plotting the pH change with the volume of titrated NaOH in Figure 4d illustrates the abrupt change from pH = 0 to pH = 5 with only 300 μ L of NaOH, while \sim 3.1 mL of NaOH is needed to shift the pH up from -1 to 0. These results clearly illustrate the need to carefully control the amount of titrant when approaching the end point in order to avoid overtitration, as well as the benefit of using a feedback control.

3.2. Software Controller

A variety of factors contribute to pH of real-world biological samples, and these factors are not universal across all samples, making the system rife with unknown processes.³⁴ With such complex samples, using a model-predictive controller would be challenging as many of the underlying parameters are not measured. Thus, a model-free controller is more suitable. Among model-free controllers, several potential candidates include an artificial neural network (ANN), a proportional integral derivative controller (PID), and a fuzzy logic controller (FLC). These control system types are compared in Table 1.

Since the pH adjustment process can be highly nonlinear, PID, which is an inherently linear controller, is less suitable to control pH titration due to the nonlinearity and uncertainty within the system. While various tuning methods for PID controllers exist, they increase computational cost, hence making the controller too sluggish to handle fast changes. Thus, an inherently nonlinear control system would likely remain preferable to an auto tuned PID.^{25,36} Furthermore,

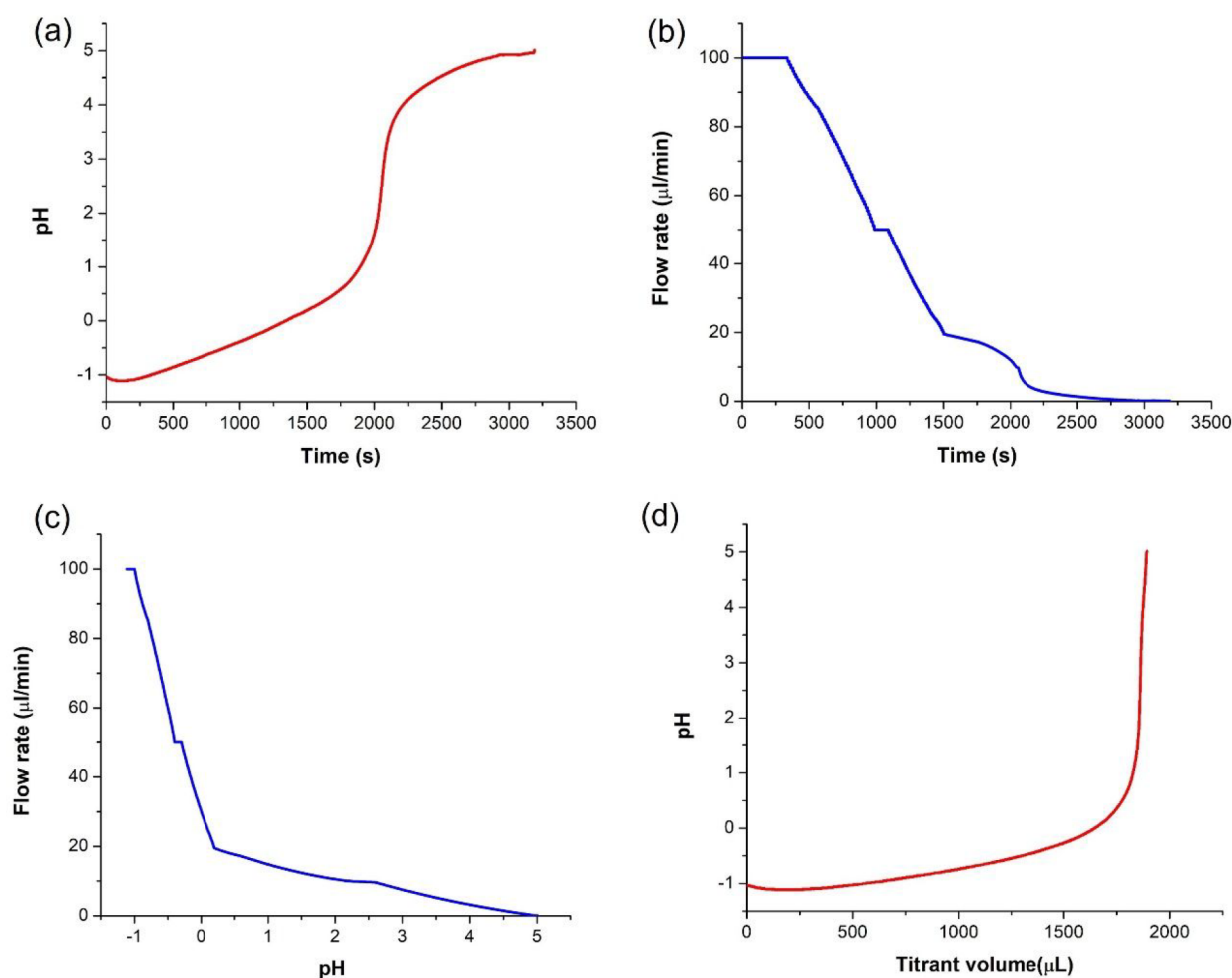


Figure 4. Representative results of automated titration. (a) pH change of the blood sample during the titration process. (b) Dispensing flow rate of NaOH titrant solution with time. (c) Dispensing flow rate of NaOH titrant solution as a function of blood sample pH. (d) pH change of the blood sample as a function of the dispensed NaOH titrant volume.

Table 1. Comparison of Key Features of the Model-Free Controllers

control system	suitable for nonlinear systems	needs precise system knowledge	training data requirements
FLC	yes ^{25,38–40,44}	no ^{25,44}	little/limited data set ^{44,37}
ANN	yes ^{25,39,40}	no ^{35,40,41}	extensive data set ^{25,35,40,41,49}
PID	no ^{25,37,38}	yes ^{37,50}	no ^{25,37}

overshoot is a significant concern in the operation of a pH titration system, and PID control systems have been found to exhibit more overshoot and perform worse than a fuzzy system.^{36–38} A likely reason for this phenomenon is that while a linear controller, such as a PID controller, can update itself to change the nonlinearities, the fuzzy logic control system has the features as a core aspect.²⁵ In addition, implementation of a PID would require more detailed system knowledge of the system, as opposed to the black box modeling controllers such as an ANN and FLC.

ANN has gained popularity in recent years and has been widely applied to various nonlinear systems.^{25,39–43} ANNs can significantly reduce the computing need and allow the use of more accurate high-order system models due to the simple mathematical expression.⁴³ Despite their incredible predictive

power, ANNs require a vast amount of training data to find a suitable ANN fit from process behavior records.^{25,40,41} This can be a significant challenge for biomedical applications due to the scarcity and high cost of the biological samples.

FLC, on the other hand, requires little data for the training phase and can be a good fit for the biomedical applications. The FLCs offer a means by which human reasoning could capture uncertainties and nonlinearities.³⁹ Their strengths lie in the ability to apply an expert's experience to a nonlinear process that is difficult to model mathematically.^{37,44} With the concept of fuzzy first proposed by Zadeh⁴⁵ in the 1960s and rapid development afterward, control systems that use fuzzy logic continued to be utilized in chemical processing, which is full of nonlinearities.²⁵ Indeed, FLCs have been established as viable controllers in both pH neutralization⁴⁴ and automation.⁴⁶

Although an FLC requires more manual tuning rules than an ANN^{39,40} and is limited in the number of input variables it can process relative to an ANN,⁴⁰ this is not a significant concern in our case. We use only two input variables (initial sample volume and the real-time pH value measured by the pH probe) and one output variable (the flow rate of the titrant), allowing for a relatively simple rule base. Another potential concern of FLCs is controller stability.^{39,47} Certain mathematical measures have been proposed to counterbalance and quantify

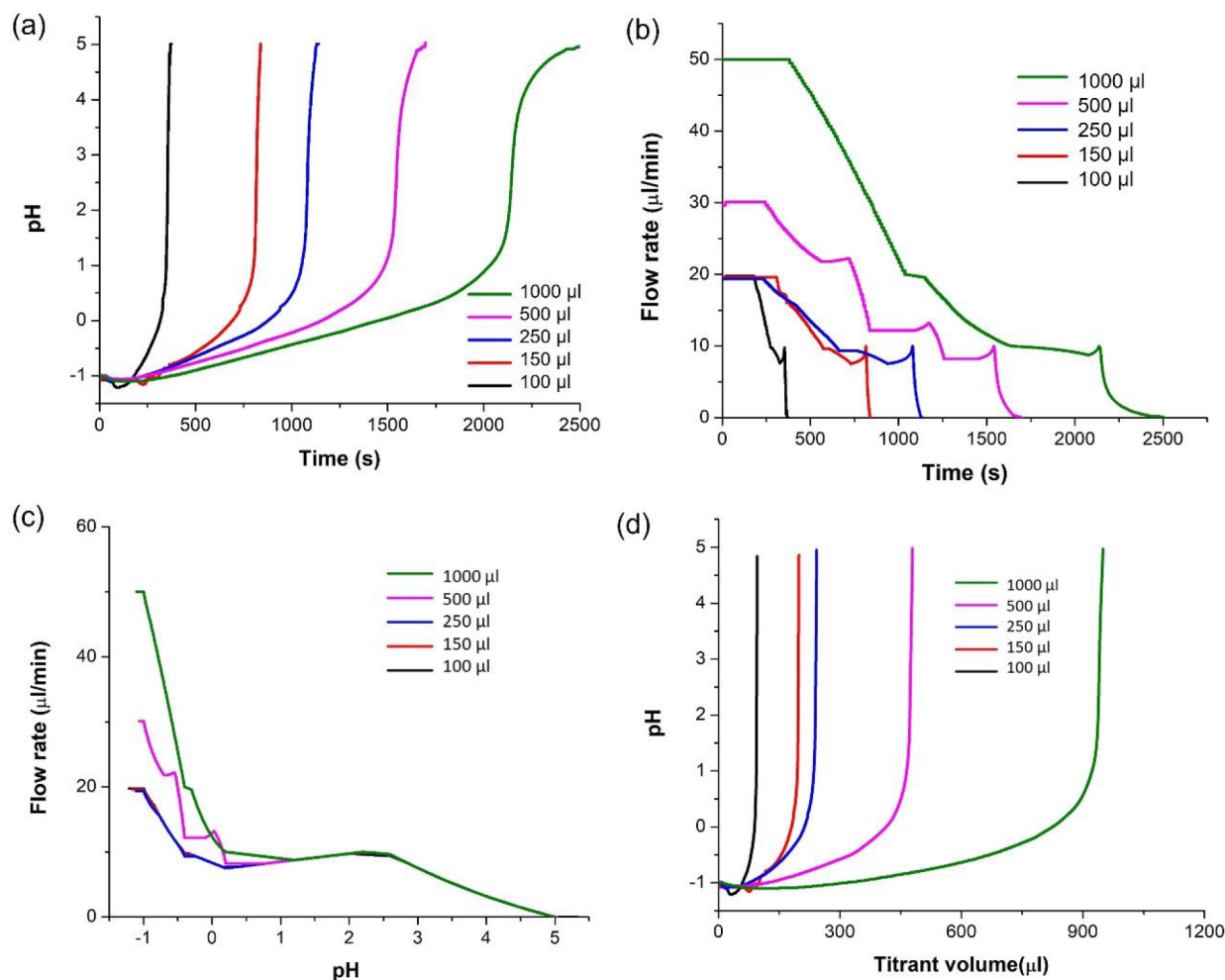


Figure 5. Representative results for autotitration of microsamples in the 100–1000 μL volume range. (a) pH change of the blood microsamples during the titration process. (b) Flow rate of the NaOH titrant solution during titration of each microvolume. (c) Flow rate of the NaOH solution with sample pH for each microvolume. (d) pH change of the blood samples with the volume of the dispensed NaOH titrant solution.

instability,³⁹ including integration with a PID controller.⁴⁷ However, the steady state response is not a significant concern of our system since the experimental setup has only one inlet, which pumps directly into a continuously stirred beaker containing the titrant. We are not concerned with a steady-state response since the blood samples simply need to be titrated to an end point for later trace-level analysis. Ultimately, based on the advantages of the FLC and the characteristics of our system, FLC was selected as the most suitable controller of our pH adjustment system.

3.3. pH Adjustment in Microvolume Samples

To demonstrate the capability of the system to work with small volumes of blood samples, we performed pH adjustments of digested blood samples in the 100 μL to 1 mL range. As Figure 5a illustrates, the microtitrator successfully adjusted the pH of all blood samples to pH = 5, including samples as low as 100 μL . The time needed for the titration process ranged from approximately 6 min for the 100 μL sample to approximately 40 min for the 1 mL sample. The majority of the time, and thus titrant volume, is spent to bring sample to pH = 0. Indeed, examining the flow rate data as a function of titration time (Figure 5b) shows that the larger the initial sample volume the longer time is spent at the higher flow rate. In these experiments, the initial flow rates were preset at 20 $\mu\text{L}/\text{min}$

for samples < 250 μL and at 50 $\mu\text{L}/\text{min}$ for the 1 mL sample. For the smallest 100 μL sample, the flow rate is downregulated in the initial 2 min, since the total titrant volume is approximately 100 μL . For the larger 1 mL sample, the titration flow rate remains at the initial preset value for nearly 10 min before being adjusted down to 20 $\mu\text{L}/\text{min}$ over the course of the following 10 min. Presetting the initial flow rate to a higher value could yield a faster titration process, although care must be taken with <250 μL samples where the initial flow rate is downregulated rapidly in order to avoid end point errors.

Plotting flow rate data as a function of sample pH (Figure 5c) illustrates that regardless of the preset initial flow rate, once pH = 0 is reached the flow rate is stabilized at 10 $\mu\text{L}/\text{min}$ until pH = 3, at which point it begins to precipitously drop until the end point is reached. This is consistent with the progression of the sample pH as a function of titrant volume (Figure 5d). As with the larger 2 mL sample discussed previously, pH values of the smaller blood samples also change abruptly with the infused NaOH for pH > 0.

3.4. Electrochemical Trace-Level Measurements in Blood Samples

Next, we applied our microtitration approach to electrochemical determination of Mn in human blood. We used the

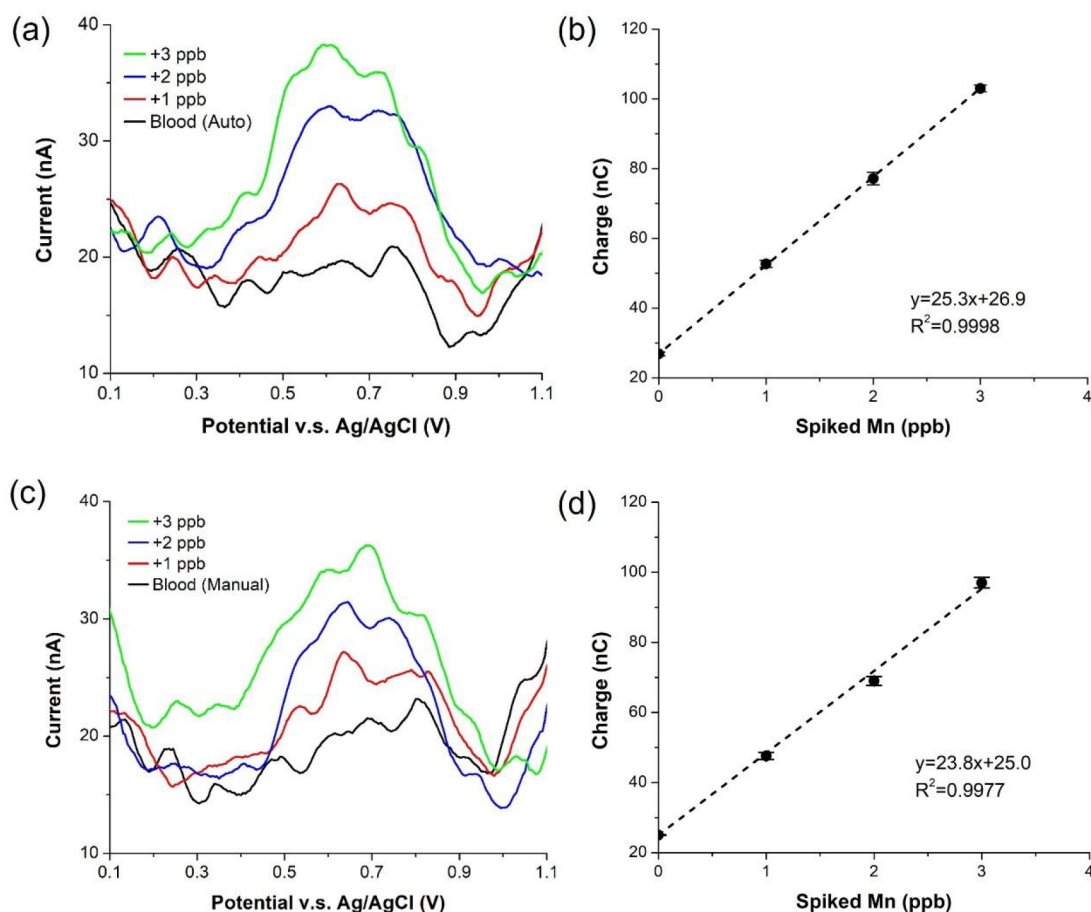


Figure 6. Comparison of results for electrochemical determination of Mn in automatically and manually adjusted pH of blood samples. (a) Representative voltammograms of the standard addition measurement for the automatically pH adjusted sample and (b) the resulting calibration curve. (c) Representative voltammograms of the standard addition measurement for the manually pH adjusted sample and (d) the resulting calibration curve.

process reported by us recently,²⁶ which involves microwave digestion of a blood sample to breakdown protein to release bound Mn and cathodic stripping on ITO electrode. To determine the unknown levels of Mn in blood, we used the standard addition approach, in which the original blood sample was spiked with 1 ppb, 2 and 3 ppb Mn. As we describe in our previous publications,^{8,26,31,48} this approach allows us to minimize matrix effects and permits accurate determination of blood Mn levels.

Representative stripping voltammograms and calibration curves for the automatically and manually adjusted samples are compared in Figure 6. In both cases, the Mn stripping peaks appear at ~ 700 mV, which is consistent with our previous results,²⁶ and exhibit similar shape and amplitude. This suggests little difference between the two samples. We measured area of the Mn peaks and did not consider measuring peak height sufficiently accurate due to peak shape. The resulting standard addition plot for the autotitrated sample (Figure 6b) provides a correlation equation of $Q(\text{nC}) = 25.3 [\text{Mn}(\text{ppb})] + 26.9$ with $R^2 = 0.9998$. The standard addition plot for the manually titrated sample (Figure 6d) yields a correlation equation of $Q(\text{nC}) = 23.8 [\text{Mn}(\text{ppb})] + 25.0$ with $R^2 = 0.9977$. Using these equations, we calculate the Mn concentration in the autoadjusted blood as 1.06 ppb and in the manually adjusted blood as 1.05 ppb. The difference in Mn concentration in the two pH-adjusted blood samples is only

0.01 ppb, which is not statically significant (Figure 7). From the comparison, we can conclude that no Mn contamination is introduced during the automated microtitration process and

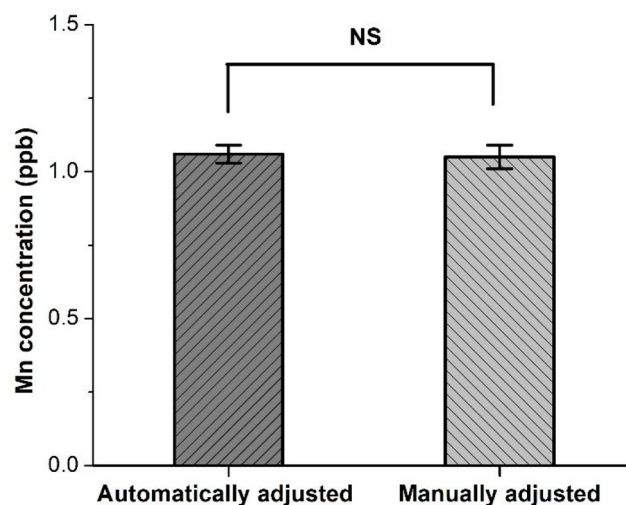


Figure 7. No significant difference in the results of automatically pH adjusted blood sample and the manually pH adjusted blood sample. A two-sample *t* test yielded no significance (NS), with $p > 0.05$ ($n = 3$).

that the use of the microtitrator is feasible for trace-level detection.

One key benefit for using the microtitrator in these measurements was the greatly reduced experiment time, in addition to a substantially lower risk of overtitration. For the Mn measurements reported above, <1 mL of the original digested blood sample was needed and the entire process could be accomplished in about 30 min. Conversely, the manual titrating process takes as much as 2 h and requires multiple pipet tips as titrant volume is progressively decreased, which increases per-sample analysis costs. As the pH change is drastic while reaching the end point, misjudgment of the titration volume can easily lead to overshooting, requiring the entire process to be repeated.

4. CONCLUSIONS

In the work, we describe an automatic microtitration system for small volume samples that are common in point-of-care and point-of-use biosample measurement applications. The system simply consists of a syringe pump for dispensing titrant and a pH microprobe for process monitoring. A fuzzy logic controller implemented in LabView instantly adjusts the dispensing flow rate of the titrant based on feedback from the pH probe. Using digested blood as the model sample, the system was successfully demonstrated to yield accurate and efficient pH adjustment for samples as small as 100 μ L. The electrochemical measurement results of Mn show that there is no detectable contamination induced by the system. Further, the modular components of the system make it compatible with acid washing for trace metal detection or cleaning to eliminate contamination. In addition, the system could also potentially be parallelized or integrated with robotic pipets for batch titrations. Ultimately, we show that the simple, accurate, user-friendly automatic microtitration system can be used in the pH adjustment of microvolume samples and can also easily be adapted to other pH end point analysis.

AUTHOR INFORMATION

Corresponding Author

Ian Papautsky – Department of Biomedical Engineering,
University of Illinois Chicago, Chicago, Illinois 60607, United States; orcid.org/0000-0002-1396-9625;
Phone: +1.312.413.3800; Email: papauts@uic.edu

Authors

Zhizhen Wu – Department of Biomedical Engineering,
University of Illinois Chicago, Chicago, Illinois 60607, United States

Abid Rehman – Department of Bioengineering, University of
Illinois Urbana-Champaign, Urbana, Illinois 61801, United States

Zhehao Zhang – Department of Biomedical Engineering,
University of Illinois Chicago, Chicago, Illinois 60607, United States

Complete contact information is available at:

<https://pubs.acs.org/10.1021/acsmeasuresci.2c00021>

Author Contributions

Z.W. and A.R. contributed equally to this work. CRediT: **Zhizhen Wu** data curation (equal), formal analysis (equal), investigation (equal), methodology (equal), writing-original draft (equal); **Abid Rehman** investigation (equal), method-

ology (equal), writing-original draft (equal); **Zhehao Zhang** investigation (equal), methodology (equal), writing-original draft (equal); **Ian Papautsky** conceptualization (lead), funding acquisition (lead), project administration (lead), supervision (lead), writing-review & editing (equal).

Notes

The authors declare no competing financial interest.

ACKNOWLEDGMENTS

This work was supported in part by funds provided by the National Institutes of Environmental Health and Sciences (NIEHS) award R33ES024717.

REFERENCES

- (1) Hutton, R. C. Application of Inductively Coupled Plasma Source Mass Spectrometry (ICP-MS) to the Determination of Trace Metals in Organics. *J. Anal. At. Spectrom.* **1986**, *1* (4), 259–263.
- (2) US EPA. *SW-846 Test Method 6020B: Inductively Coupled Plasma - Mass Spectrometry*. <https://www.epa.gov/hw-sw846/sw-846-test-method-6020b-inductively-coupled-plasma-mass-spectrometry> (accessed 2022-04-18).
- (3) Smith, J. C.; Butrimovitz, G. P.; Purdy, W. C. Direct Measurement of Zinc in Plasma by Atomic Absorption Spectroscopy. *Clin. Chem.* **1979**, *25* (8), 1487–1491.
- (4) Willis, J. B. Determination of Calcium and Magnesium in Urine by Atomic Absorption Spectroscopy. *Anal. Chem.* **1961**, *33* (4), 556–559.
- (5) Rehkämper, M.; Schönbachler, M.; Stirling, C. H. Multiple Collector ICP-MS: Introduction to Instrumentation, Measurement Techniques and Analytical Capabilities. *Geostand. Newsl.* **2001**, *25* (1), 23–40.
- (6) Hwang, J.-H.; Pathak, P.; Wang, X.; Rodriguez, K. L.; Cho, H. J.; Lee, W. H. A Novel Bismuth-Chitosan Nanocomposite Sensor for Simultaneous Detection of Pb(II), Cd(II) and Zn(II) in Wastewater. *Micromachines* **2019**, *10* (8), 511.
- (7) Rusinek, C. A.; Bange, A.; Warren, M.; Kang, W.; Nahan, K.; Papautsky, I.; Heineman, W. R. Bare and Polymer-Coated Indium Tin Oxide as Working Electrodes for Manganese Cathodic Stripping Voltammetry. *Anal. Chem.* **2016**, *88* (8), 4221–4228.
- (8) Kang, W.; Pei, X.; Bange, A.; Haynes, E. N.; Heineman, W. R.; Papautsky, I. Copper-Based Electrochemical Sensor with Palladium Electrode for Cathodic Stripping Voltammetry of Manganese. *Anal. Chem.* **2014**, *86* (24), 12070–12077.
- (9) Jothimuthu, P.; Wilson, R. A.; Herren, J.; Haynes, E. N.; Heineman, W. R.; Papautsky, I. Lab-on-a-Chip Sensor for Detection of Highly Electronegative Heavy Metals by Anodic Stripping Voltammetry. *Biomed. Microdevices* **2011**, *13* (4), 695–703.
- (10) Pei, X.; Kang, W.; Yue, W.; Bange, A.; Heineman, W. R.; Papautsky, I. Disposable Copper-Based Electrochemical Sensor for Anodic Stripping Voltammetry. *Anal. Chem.* **2014**, *86* (10), 4893–4900.
- (11) Gao, W.; Nyein, H. Y. Y.; Shahpar, Z.; Fahad, H. M.; Chen, K.; Emaminejad, S.; Gao, Y.; Tai, L.-C.; Ota, H.; Wu, E.; Bullock, J.; Zeng, Y.; Lien, D.-H.; Javey, A. Wearable Microsensor Array for Multiplexed Heavy Metal Monitoring of Body Fluids. *ACS Sens.* **2016**, *1* (7), 866–874.
- (12) Shen, L.-L.; Zhang, G.-R.; Li, W.; Biesalski, M.; Etzold, B. J. M. Modifier-Free Microfluidic Electrochemical Sensor for Heavy-Metal Detection. *ACS Omega* **2017**, *2* (8), 4593–4603.
- (13) Li, S.; Zhang, C.; Wang, S.; Liu, Q.; Feng, H.; Ma, X.; Guo, J. Electrochemical Microfluidics Techniques for Heavy Metal Ion Detection. *Analyst* **2018**, *143* (18), 4230–4246.
- (14) Rusinek, C. A.; Bange, A.; Papautsky, I.; Heineman, W. R. Cloud Point Extraction for Electroanalysis: Anodic Stripping Voltammetry of Cadmium. *Anal. Chem.* **2015**, *87* (12), 6133–6140.

- (15) Wright, R. A.; Kravaris, C. Nonlinear Control of PH Processes Using the Strong Acid Equivalent. *Ind. Eng. Chem. Res.* **1991**, *30* (7), 1561–1572.
- (16) Automatic Potentiometric (pH/mV/ISE) Titration System - HI902C. <https://www.hannainst.com/hi902c-automatic-titration-system.html> (accessed 2022-03-11).
- (17) Orion Star T910 pH Titrator and Kits. <https://www.thermofisher.com/order/catalog/product/START9100> (accessed 2022-03-11).
- (18) Mettler Toledo. *Titrators*. https://www.mt.com/us/en/home/products/Laboratory_Analytics_Browse/Product_Family_Browse_titrators_main.html (accessed 2022-03-11).
- (19) Segara, F.; Kobayashi, T.; Tajima, T.; Ijyuuin, H.; Yoshida, I.; Ishii, D.; Ueno, K. Development of a Micro Flow Spectrophotometric Titration Method. *Anal. Chim. Acta* **1992**, *261* (1), 505–508.
- (20) Gros, N. A New Type of a Spectrometric Microtitration Set Up. *Talanta* **2005**, *65* (4), 907–912.
- (21) Li, Q.; Wang, F.; Wang, Z. A.; Yuan, D.; Dai, M.; Chen, J.; Dai, J.; Hoering, K. A. Automated Spectrophotometric Analyzer for Rapid Single-Point Titration of Seawater Total Alkalinity. *Environ. Sci. Technol.* **2013**, *47* (19), 11139–11146.
- (22) van der Schoot, B.; van der Wal, P.; de Rooij, N.; West, S. Titration-on-a-Chip, Chemical Sensor-Actuator Systems from Idea to Commercial Product. *Sens. Actuators B Chem.* **2005**, *105* (1), 88–95.
- (23) Steinsberger, T.; Kathriner, P.; Meier, P.; Mistretta, A.; Hauser, P. C.; Müller, B. A Portable Low Cost Coulometric Micro-Titrator for the Determination of Alkalinity in Lake and Sediment Porewaters. *Sens. Actuators B Chem.* **2018**, *255*, 3558–3563.
- (24) Chen, Y.; Li, X.; Li, D.; Batchelor-McAuley, C.; Compton, R. G. A Simplified Methodology: PH Sensing Using an in Situ Fabricated Ir Electrode under Neutral Conditions. *J. Solid State Electrochem.* **2021**, *25* (12), 2821–2833.
- (25) Hermansson, A. W.; Syafie, S. Model Predictive Control of PH Neutralization Processes: A Review. *Control Eng. Pract.* **2015**, *45*, 98–109.
- (26) Wu, Z.; Heineman, W. R.; Haynes, E. N.; Papautsky, I. Electrochemical Determination of Manganese in Whole Blood with Indium Tin Oxide Electrode. *J. Electrochem. Soc.* **2022**, *169* (5), 057508.
- (27) Zhang, Z.; Papautsky, I. Solid Contact Ion-Selective Electrodes on Printed Circuit Board with Membrane Displacement. *Electroanalysis* **2022**, DOI: 10.1002/elan.202100686.
- (28) Tan, A.; Zhang, L.; Xiao, C. Simultaneous and Automatic Determination of Hydroxide and Carbonate in Aluminate Solutions by a Micro-Titration Method. *Anal. Chim. Acta* **1999**, *388* (1), 219–223.
- (29) Kozak, J.; Paluch, J.; Kozak, M.; Duracz, M.; Wieczorek, M.; Kościelniak, P. Novel Approach to Automated Flow Titration for the Determination of Fe(III). *Molecules* **2020**, *25* (7), 1533.
- (30) Pereiro, I.; Fomitcheva-Khartchenko, A.; Kaigala, G. V. Shake It or Shrink It: Mass Transport and Kinetics in Surface Bioassays Using Agitation and Microfluidics. *Anal. Chem.* **2020**, *92* (15), 10187–10195.
- (31) Kang, W.; Rusinek, C.; Bange, A.; Haynes, E.; Heineman, W. R.; Papautsky, I. Determination of Manganese by Cathodic Stripping Voltammetry on a Microfabricated Platinum Thin-Film Electrode. *Electroanalysis* **2017**, *29* (3), 686–695.
- (32) Boselli, E.; Wu, Z.; Friedman, A.; Claus Henn, B.; Papautsky, I. Validation of Electrochemical Sensor for Determination of Manganese in Drinking Water. *Environ. Sci. Technol.* **2021**, *55* (11), 7501–7509.
- (33) Rusinek, C. A.; Kang, W.; Nahan, K.; Hawkins, M.; Quartermaine, C.; Stastny, A.; Bange, A.; Papautsky, I.; Heineman, W. R. Determination of Manganese in Whole Blood by Cathodic Stripping Voltammetry with Indium Tin Oxide. *Electroanalysis* **2017**, *29* (8), 1850–1853.
- (34) Kellum, J. A. Determinants of Blood PH in Health and Disease. *Crit. Care London Engl.* **2000**, *4* (1), 6–14.
- (35) Klein, A. Challenges of Model Predictive Control in a Black Box Environment. In *Reinforcement Learning Algorithms: Analysis and Applications*; Belousov, B., Abdulsamad, H., Klink, P., Parisi, S., Peters, J., Eds.; Studies in Computational Intelligence; Springer International Publishing: Cham, 2021; pp 177–187. DOI: 10.1007/978-3-030-41188-6_15.
- (36) Bhandare, D. S.; Kulkarni, N. R. Performances Evaluation and Comparison of PID Controller and Fuzzy Logic Controller for Process Liquid Level Control. In *2015 15th International Conference on Control, Automation and Systems (ICCAS)*; 2015; pp 1347–1352. DOI: 10.1109/ICCAS.2015.7364848.
- (37) Chung, C.-C.; Chen, H.-H.; Ting, C.-H. Grey Prediction Fuzzy Control for PH Processes in the Food Industry. *J. Food Eng.* **2010**, *96* (4), 575–582.
- (38) Chao, C.-T.; Sutarna, N.; Chiou, J.-S.; Wang, C.-J. Equivalence between Fuzzy PID Controllers and Conventional PID Controllers. *Appl. Sci.* **2017**, *7* (6), 513.
- (39) Jiang, Y.; Yang, C.; Ma, H. A Review of Fuzzy Logic and Neural Network Based Intelligent Control Design for Discrete-Time Systems. *Discrete Dyn. Nat. Soc.* **2016**, *2016*, 7217364.
- (40) Pezeshki, Z.; Mazinani, S. M. Comparison of Artificial Neural Networks, Fuzzy Logic and Neuro Fuzzy for Predicting Optimization of Building Thermal Consumption: A Survey. *Artif. Intell. Rev.* **2019**, *52* (1), 495–525.
- (41) Marcus, G.; Davis, E. *Rebooting AI: Building Artificial Intelligence We Can Trust*; Pantheon Books, 2019.
- (42) Shin, Y.; Smith, R.; Hwang, S. Development of Model Predictive Control System Using an Artificial Neural Network: A Case Study with a Distillation Column. *J. Clean. Prod.* **2020**, *277*, 124124.
- (43) Wang, D.; Shen, Z. J.; Yin, X.; Tang, S.; Liu, X.; Zhang, C.; Wang, J.; Rodriguez, J.; Norambuena, M. Model Predictive Control Using Artificial Neural Network for Power Converters. *IEEE Trans. Ind. Electron.* **2022**, *69* (4), 3689–3699.
- (44) Arun, U. P.; George, S.; Mobeen, S. A. Control of PH Neutralization Process Using Fuzzy Logic: A Review. *Int. Res. J. Eng. Technol.* **2015**, *2* (3), 1081.
- (45) Zadeh, L. A. Fuzzy Sets. *Inf. Control* **1965**, *8* (3), 338–353.
- (46) Nascimento, T. P.; Saska, M. Position and Attitude Control of Multi-Rotor Aerial Vehicles: A Survey. *Annu. Rev. Control* **2019**, *48*, 129–146.
- (47) Naseer, O.; Khan, A. A. Hybrid Fuzzy Logic and Pid Controller Based Ph Neutralization Pilot Plant. *Int. J. Fuzzy Syst.* **2013**, *3* (2), 1.
- (48) Jothimuthu, P.; Wilson, R. A.; Herren, J.; Pei, X.; Kang, W.; Daniels, R.; Wong, H.; Beyette, F.; Heineman, W. R.; Papautsky, I. Zinc Detection in Serum by Anodic Stripping Voltammetry on Microfabricated Bismuth Electrodes. *Electroanalysis* **2013**, *25* (2), 401–407.
- (49) Sena, H. J.; Silva, F. V. da; Fileti, A. M. F. ANN Model Adaptation Algorithm Based on Extended Kalman Filter Applied to PH Control Using MPC. *J. Process Control* **2021**, *102*, 15–23.
- (50) Pelusi, D.; Mascella, R. Optimal Control Algorithms for Second Order Systems. *J. Comput. Sci.* **2013**, *9* (2), 183–197.